Severe 2011 ozone depletion assessed with 11 years of ozone, NO_2, and OClO measurements at 80°N

C. Adams,[1] K. Strong,[1] X. Zhao,[1] M. R. Bassford,[1,2] M. P. Chipperfield,[3] W. Daffer,[4] J. R. Drummond,[1,5] E. E. Farahani,[1] W. Feng,[3,6] A. Fraser,[1,7] F. Goutail,[8] G. Manney,[4,9] C. A. McLinden,[10] A. Pazmino,[8] M. Rex,[11] and Kaley A. Walker[1,12]

Received 4 December 2011; revised 7 February 2012; accepted 14 February 2012; published 13 March 2012.

[1] Unusually cold conditions in Arctic winter 2010/11 led to large stratospheric ozone loss. We investigate this with UV-visible measurements made at Eureka, Canada (80.05°N, 86.42°W) from 1999–2011. For 8–22 March 2011, OClO was enhanced, indicating chlorine activation above Eureka. Ozone columns were lower than in any other year in the record, reaching minima of 237 DU and 247 DU in two datasets. The average NO_2 column inside the vortex, measured at visible and UV wavelengths, was 46 ± 30% and 45 ± 27% lower in 2011 than the average NO_2 column from previous years. Ozone column loss was estimated from two ozone datasets, using a modeled passive ozone tracer. For 12–20 March 2011, the average ozone loss was 27% and 29% (99 DU and 108 DU). The largest percent ozone loss in the 11-year record of 47% (250 DU and 251 DU) was observed on 5 April 2011. **Citation:** Adams, C., et al. (2012), Severe 2011 ozone depletion assessed with 11 years of ozone, NO_2, and OClO measurements at 80°N, *Geophys. Res. Lett.*, *39*, L05806, doi:10.1029/2011GL050478.

1. Introduction

[2] In spring 2011, chemical ozone loss in the Arctic was comparable to that observed over Antarctica for the first time on record [*Manney et al.*, 2011]. This resulted from an unusually prolonged period with a strong, cold polar vortex. Due to these persistent low temperatures, polar stratospheric clouds (PSCs) were observed until mid-March and activated chlorine was observed until late March. This resulted in a record ozone loss [*Balis et al.*, 2011; *Manney et al.*, 2011].

[3] The polar vortex was above the Polar Environment Atmospheric Research Laboratory (PEARL), located at Eureka, Canada (80.05°N, 86.42°W) for a large part of spring 2011. A suite of instruments, operated by the Canadian Network for the Detection of Atmospheric Change (CANDAC), take continuous measurements at PEARL. We present results from four differential optical absorption spectroscopy (DOAS) instruments. DOAS instruments can measure under both clear and cloudy conditions and therefore present a more continuous timeseries of ozone and NO_2 than solar tracking Fourier Transform Infrared (FTIR) spectrometers. Furthermore, DOAS instruments can also measure OClO, which is a good qualitative indicator of chlorine activation [*Sessler et al.*, 1995]. However, quantification of ClO from OClO measurements is difficult due to uncertainties in model predictions, particularly under strong chlorine activation [e.g., *Oetjen et al.*, 2011]. Ozone, NO_2, and OClO measurements can be combined with stratospheric parameters in order to identify ozone depletion, chlorine activation, and denitrification within the polar vortex [e.g., *Tornkvist et al.*, 2002; *Tétard et al.*, 2009].

2. Datasets

[4] Measurements included in this study were taken by four ground-based DOAS instruments: the PEARL and University of Toronto ground-based spectrometers (GBSs) [*Fraser et al.*, 2009] and two System D'Analyse par Observations Zenithales (SAOZ) instruments [*Pommereau and Goutail*, 1988]. These instruments are part of the Network for the Detection of Atmospheric Composition Change (NDACC) and their Eureka ozone and NO_2 datasets are described in detail by *Adams et al.* [2012]. Measurements from the two GBS (two SAOZ) instruments are nearly identical and therefore were combined to create a single GBS (SAOZ) dataset.

[5] The GBSs are UV-visible Triax-180 triple-grating spectrometers, built by Instruments S.A. / Jobin Yvon Horiba, with cooled charge-coupled device detectors and a 2° field-of-view. The resolution varies from 0.2–2.5 nm and the wavelength range varies from 320–600 nm depending on the selected grating and target wavelength. GBS ozone and NO_2 columns were retrieved above Eureka in the spring for 1999–2011, except for 2001 and 2002. The SAOZ instruments are grating spectrometers, which measure in the 270–620 nm range with a 1.0-nm resolution and a 10° field-

[1]Department of Physics, University of Toronto, Toronto, Ontario, Canada.
[2]Now at RAND Europe, Cambridge, UK.
[3]Institute for Climate and Atmospheric Science, School of Earth and Environment, University of Leeds, Leeds, UK.
[4]Jet Propulsion Laboratory, California Institute of Technology, Pasadena, California, USA.
[5]Department of Physics and Atmospheric Sciences, Dalhousie University, Halifax, Nova Scotia, Canada.
[6]National Centre for Atmospheric Science, School of Earth and Environment, University of Leeds, Leeds, UK.
[7]Now at School of GeoSciences, University of Edinburgh, Edinburgh, UK.
[8]LATMOS, CNRS, Guyancourt, France.
[9]Department of Physics, New Mexico Institute of Mining and Technology, Socorro, New Mexico, USA.
[10]Environment Canada, Toronto, Ontario, Canada.
[11]Alfred Wegener Institute for Polar and Marine Research, Potsdam, Germany.
[12]Department of Chemistry, University of Waterloo, Waterloo, Ontario, Canada.

0094-8276/12/2011GL050478

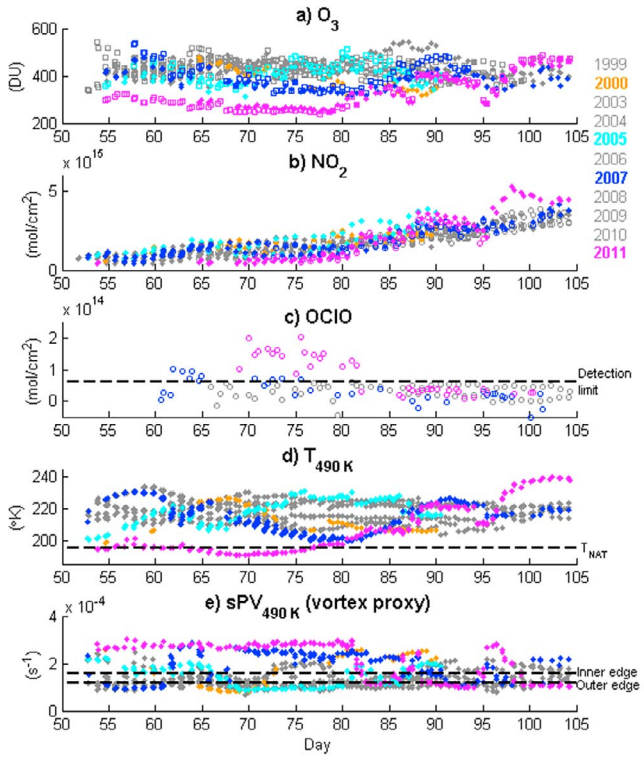

Figure 1. Timeseries of measurements and dynamical parameters along the DOAS line-of-sight for 1999–2011 versus day of year. Year 2000 is shown in orange, 2005 in cyan, 2007 in blue, 2011 in magenta, and all other years are shown in grey. (a) Ozone total columns measured by the GBS (closed diamonds) and SAOZ (open squares). (b) NO_2 partial columns (17 km to top of atmosphere) measured by GBS-vis (closed diamonds) and GBS-UV (open circles). (c) OClO DSCDs measured by the GBS. (d) T_{490K} and (e) sPV_{490K}.

of-view and record spectra on uncooled 1024-pixel linear diode array detectors. SAOZ instruments took spring-time measurements at Eureka for 2005–2011.

[6] The DOAS (GBS and SAOZ) ozone measurements were analyzed in the 450–550 nm range, using the NDACC guidelines [*Hendrick et al.*, 2011]. NO_2 partial columns were retrieved for the GBS instruments in two different wavelength regions: 425–450 nm (GBS-vis) and 350–380 nm (GBS-UV), depending on the selected measurement grating. The GBS NO_2 partial columns were calculated for 17 km to the top of the atmosphere for the validation of satellite partial column measurements, using AMFs that were set to zero below 17 km [*Adams et al.*, 2012]. SAOZ NO_2 total columns were retrieved in the 410–510 nm range. The SAOZ NO_2 total columns are qualitatively consistent with the GBS partial columns, but are not presented here because they cover a different altitude range. The SAOZ and GBS ozone and NO_2 columns have been shown to agree well with other ground-based and satellite measurements [*Fraser et al.*, 2008, 2009; *Adams et al.*, 2012]. OClO differential slant column densities (DSCDs) at solar zenith angle 90° were also retrieved from spring 2007, 2008, and 2011 GBS spectra in the 350–380 nm range. The OClO retrievals are described in the auxiliary material.[1]

[7] Derived meteorological products [*Manney et al.*, 2007] were calculated along the lines-of-sight of the DOAS instruments [*Adams et al.*, 2012] for 1999–2003 using the Met Office analysis and 2004–2011 using the GEOS-5.1.0/GEOS-5.2.0 analysis. Stratospheric temperatures and scaled potential vorticity (sPV) were interpolated to the 490-K potential temperature level (∼ ozone concentration maximum, ∼19 km) and are referred to here as T_{490K} and sPV_{490K}. The inner and outer vortex edges are identified by sPV_{490K} values of 1.6×10^{-4} s^{-1} and 1.2×10^{-4} s^{-1}, respectively [*Manney et al.*, 2007].

3. Timeseries of Ozone, NO_2, and OClO

[8] The 1999–2011 timeseries of ozone, NO_2, OClO, T_{490K}, and sPV_{490K} are shown in Figure 1. In 2000, 2005, 2007 and 2011, low ozone columns were measured above Eureka when the polar vortex was overhead. These years are shown in color, while the other measurement years are shown in grey. Low ozone coincides with low NO_2, low T_{490K}, and time periods when the instruments are sampling inside the polar vortex.

[9] For 23 February to 21 March 2011 (days 54–80), the DOAS instruments sample lower stratospheric air inside the polar vortex. OClO DSCDs of $0.8–2.0 \times 10^{14}$ mol/cm^2 are within the range of previous elevated OClO measurements [e.g., *Tornkvist et al.*, 2002], suggesting chlorine activation. All elevated OClO DSCDs, from 8–22 March 2011 (days 67–81) and 2–5 March 2007 (days 61–64), are measured inside the polar vortex when the high-latitude minimum temperature (calculated by *Manney et al.* [2011], not shown here) is below the threshold for PSC formation (T_{NAT}). High OClO measurements do not always correspond with local $T_{490K} < T_{NAT}$ (Figure 1d), because the time-scale for vortex mixing (∼5–7 days) is smaller than the time-scale for chlorine deactivation (∼weeks). During the period of elevated OClO in 2011, ozone, NO_2, and T_{490K} all reach minima in the 11-year record, with ozone values of 247 DU (237 DU) measured by the GBS (SAOZ) on 18 March (day 77).

[10] After 22 March 2011 (day 81), the instruments primarily sample the lower stratosphere outside the polar vortex. During this period, ozone and NO_2 increase to levels that are normal in the context of the 11-year data record. On 5 April (day 87) and 28 March (day 95), ozone and NO_2 columns and T_{490K} decrease sharply, as the instruments sample air masses inside the vortex. After 5 April (day 95), T_{490K} and NO_2 increase to maxima in the 11-year dataset. This increase is the subject of a companion study.

4. Dynamical and Chemical Contributions to Low Ozone

[11] As is evident in the DOAS timeseries (Figure 1), 2011 is extremely different from previous years. Ozone, NO_2, and OClO measurements taken inside the polar vortex ($sPV_{490K} > 1.6 \times 10^{-4}$ s^{-1}) for days 55–80 (24 February to 19/20 March) were selected to investigate this further. The time-period was limited in order to reduce the impact of

[1]Auxiliary materials are available in the HTML. doi:10.1029/2011GL050478.

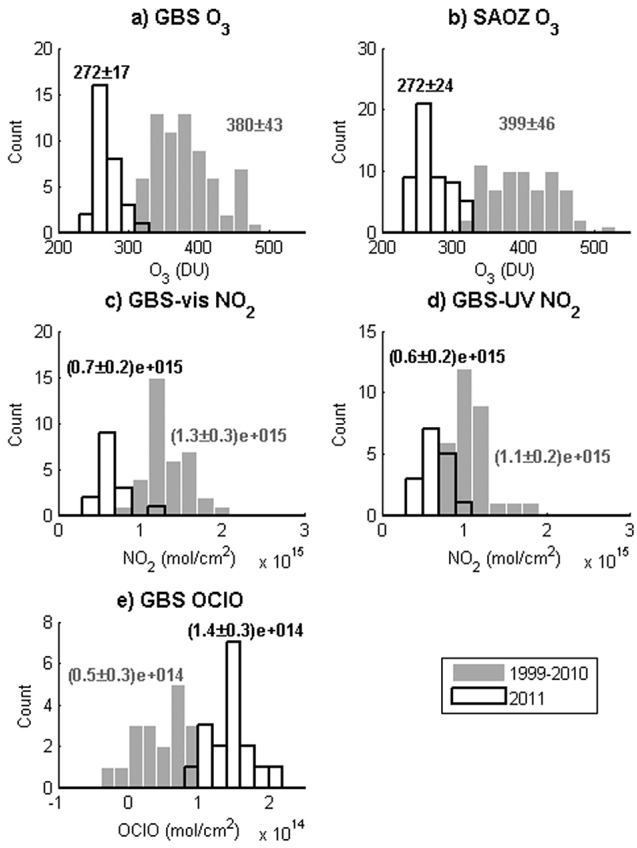

Figure 2. Histograms of (a) GBS ozone, (b) SAOZ ozone, (c) GBS-vis NO_2, (d) GBS-UV NO_2, and (e) GBS OClO. Measurements were taken inside the vortex for days 55–80 (24 February to 19/20 March), with 1999–2010 in gray and 2011 transparent with thick black lines. N ± M denotes the average (N) and 1σ standard deviation (M) in the measurements.

seasonal variation on the results. NO_2 measurements were scaled to local solar noon using a photochemical model [*McLinden et al.*, 2000] initialized with temperature and ozone from Eureka ozonesonde profiles from the nearest available date.

[12] Figure 2 shows histograms of ozone, NO_2, and OClO for 1999–2010 (grey) and 2011 (transparent with thick black outline). In 2011, the mean vortex ozone column measured by the GBS (SAOZ) is 28 ± 13% (32 ± 14%) lower than the mean column from other years, where the error denotes the 1σ statistical uncertainty. Similarly, GBS-vis (GBS-UV) NO_2 is 46 ± 30% (45 ± 27%) lower and GBS OClO is three times higher in 2011 than in previous years.

[13] The unusual 2011 ozone and NO_2 columns are a result of both chemistry and transport, which contribute approximately equally to year-to-year total ozone column variability in the Arctic [*Tegtmeier et al.*, 2008]. Figure 3 shows the correlation between vortex ozone/NO_2 measurements and the local T_{490K}. Correlation between ozone and local lower stratospheric temperature has been observed in previous studies and points to replenishing of ozone through vertical descent, horizontal mixing across the vortex edge, and adiabatic compression of the column, which all increase with higher stratospheric temperatures (e.g., supplementary material of *Manney et al.* [2011, and references therein]). In the present study, the strongest correlation between ozone and T_{490K} was calculated when data were excluded from years with few vortex measurements above Eureka (grey) and 12–20 March 2011 (days 71–79, red). The outliers for years with few vortex measurements may result from errors in matching T_{490K} and sPV_{490K} to measurements both spatially and temporally when the vortex edge is near Eureka. For 12–20 March 2011, the ozone columns remain low, despite the rise in the local T_{490K}. This deviation from the correlation between T_{490K} and ozone suggests chemical depletion (supplementary material of *Manney et al.* [2011]). NO_2 is also correlated with local lower stratospheric temperature, as has been observed in previous studies [e.g., *Pommereau and Goutail*, 1988; *Dirksen et al.*, 2011]. The correlation for NO_2 is weaker than for ozone, likely due to the seasonal increase in NO_2 as it is released from night-time reservoirs.

[14] Investigation of complementary datasets provides further evidence of chemical ozone depletion and denitrification above Eureka in 2011. For 9–18 March (days 68–77), low HNO_3 and $ClONO_2$ columns over Eureka were measured by the CANDAC Bruker FTIR [*Lindenmaier et al.*, 2012]. This suggests that the extremely low NO_2 columns measured during the same period are not caused by conversion to HNO_3 or $ClONO_2$. During this period of low $ClONO_2$, HNO_3, and NO_2, OClO DSCDs are elevated, reinforcing that chlorine remains activated. Furthermore, PSCs were measured above Eureka with the CANDAC

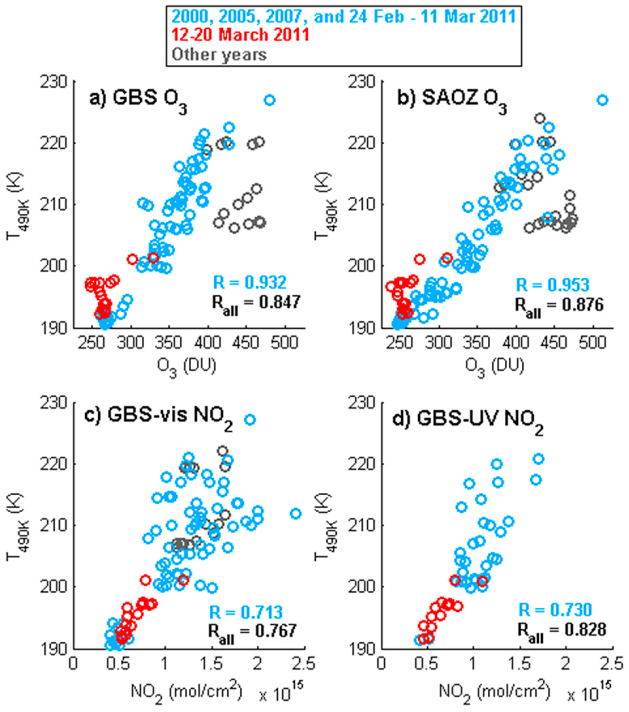

Figure 3. Correlation between T_{490K} and (a) GBS ozone, (b) SAOZ ozone, (c) GBS-vis NO_2, and (d) GBS-UV NO_2. Measurements were taken inside the vortex for days 55–80 (24 February to 19/20 March). Data are shown for 2000, 2005, 2007, and 24 February to 11 March 2011 (blue); 12–20 March 2011 (red); and other years (grey). R and R_{all} are correlation coefficients for data indicated by blue only and for all data in the figure, respectively.

Rayleigh-Mie-Raman Lidar between 8–18 March (days 67–77) [*Lindenmaier et al.*, 2012]. These measurements agree with photochemical model runs in supplementary material of *Manney et al.* [2011], which indicate that prolonged denitrification by sedimentation of PSCs delayed chlorine deactivation, leading to the record ozone loss.

[15] In order to isolate chemical ozone depletion from dynamical features, the passive subtraction method [e.g., *Manney et al.*, 1995; *World Meteorological Organization*, 2003; *Feng et al.*, 2007] was employed using SLIMCAT [*Chipperfield*, 2006], a three-dimensional off-line chemical transport model. These ozone loss estimates are described in detail in the auxiliary material. The average ozone loss for 12–20 March 2011 was 27% (29%) or 99 DU (108 DU), as estimated from GBS (SAOZ) data. The maximum percent ozone loss in the 11-year data record was calculated from GBS (SAOZ) data on 5 April 2011 at 47% (47%) or 250 DU (251 DU). A similar maximum ozone loss of 266 DU was observed by *Lindenmaier et al.* [2012] on 5 April 2011 above Eureka.

5. Conclusion

[16] Unprecedentedly low ozone and NO_2 columns were measured in 2011 and correspond to elevated OClO, suggesting chlorine activation and ozone depletion. Vortex ozone and NO_2 total columns from 1999–2011 are correlated with the lower stratospheric temperature above Eureka, indicating that transport also contributes to the low ozone and NO_2 measurements. Using the SLIMCAT passive tracer model, a maximum percent ozone loss of 47% was observed on 5 April 2011.

[17] **Acknowledgments.** The 2006–2011 GBS measurements were made at PEARL by CANDAC. CANDAC is supported by the Atlantic Innovation Fund/Nova Scotia Research Innovation Trust, Canada Foundation for Innovation, Canadian Foundation for Climate and Atmospheric Sciences (CFCAS), Canadian Space Agency (CSA), Environment Canada (EC), Government of Canada International Polar Year funding, Natural Sciences and Engineering Research Council (NSERC), Northern Scientific Training Program (NSTP), Ontario Innovation Trust, Polar Continental Shelf Program, and Ontario Research Fund. Ozonesonde measurements were made by EC. The spring 2004–2011 GBS, SAOZ, and ozonesonde measurements were also supported by the Canadian Arctic ACE Validation Campaigns, which were funded by CSA, NSERC, NSTP, EC, and the Centre for Global Change Science. The spring 1999–2000 GBS measurements were supported by NSERC and the University of Toronto and the 2001–2003 GBS measurements were supported by CFCAS and NSTP. SAOZ participation in the campaigns was supported by the Centre National D'Études Spatiales. The authors wish to thank PEARL site manager Pierre F. Fogal, the CANDAC operators, and the staff at EC's Eureka weather station for their contributions to data acquisition, and logistical and on-site support. Work carried out at the Jet Propulsion Laboratory, California Institute of Technology was done under contract with the National Aeronautics and Space Administration. The QDOAS data analysis software and ozone/NO_2 air-mass factors were provided by IASB-BIRA.

[18] The Editor thanks Hideaki Nakajima and an anonymous reviewer for their assistance in evaluating this paper.

References

Adams, C., et al. (2012), Validation of ACE and OSIRIS ozone and NO_2 measurements using ground-based instruments at 80°N, *Atmos. Meas. Tech. Discuss.*, *5*, 517–588, doi:10.5194/amtd-5-517-2012.

Balis, D., et al. (2011), Observed and modelled record ozone decline over the Arctic during winter/spring 2011, *Geophys. Res. Lett.*, *38*, L23801, doi:10.1029/2011GL049259.

Chipperfield, M. P. (2006), New version of the TOMCAT/SLIMCAT off-line chemical transport model: Intercomparison of stratospheric tracer experiments, *Q. J. R. Meteorol. Soc.*, *132*, 1179–1203, doi:10.1256/qj.05.51.

Dirksen, R. J., K. F. Boersma, H. J. Eskes, D. V. Ionov, E. J. Bucsela, P. F. Levelt, and H. M. Kelder (2011), Evaluation of stratospheric NO_2 retrieved from the Ozone Monitoring Instrument: Intercomparison, diurnal cycle, and trending, *J. Geophys. Res.*, *116*, D08305, doi:10.1029/2010JD014943.

Feng, W., M. P. Chipperfield, S. Davies, P. von der Gathen, E. Kyrö, C. M. Volk, A. Ulanovsky, and G. Belyaev (2007), Large chemical ozone loss in 2004/05 Arctic winter/spring, *Geophys. Res. Lett.*, *34*, L09803, doi:10.1029/2006GL029098.

Fraser, A., et al. (2008), Intercomparison of UV-visible measurements of ozone and NO_2 during the Canadian Arctic ACE validation campaigns: 2004–2006, *Atmos. Chem. Phys.*, *8*, 1763–1788, doi:10.5194/acp-8-1763-2008.

Fraser, A., et al. (2009), The Polar Environment Atmospheric Research Laboratory UV-visible ground-based spectrometer: first measurements of O_3, NO_2, BrO, and OClO columns, *J. Quant. Spectrosc. Radiat. Transfer*, *110*, 986–1004, doi:10.1016/j.jqsrt.2009.02.034.

Hendrick, F., et al. (2011), NDACC/SAOZ UV-visible total ozone measurements: improved retrieval and comparison with correlative satellite and ground-based observations, *Atmos. Chem. Phys.*, *11*, 5975–5995, doi:10.5194/acp-11-5975-2011.

Lindenmaier, R., et al. (2012), Unusually low ozone, HCl, and HNO_3 column measurements at Eureka, Canada during winter/spring 2011, *Atmos. Chem. Phys. Discuss.*, *12*, 1053–1092, doi:10.5194/acpd-12-1053-2012.

Manney, G. L., et al. (1995), Lagrangian transport calculations using UARS data. 2. Ozone, *J. Atmos. Sci.*, *52*, 3069–3081, doi:10.1175/1520-0469(1995)052<3069:LTCUDP>2.0.CO;2.

Manney, G. L., et al. (2007), Solar occultation satellite data and derived meteorological products: Sampling issues and comparisons with Aura Microwave Limb Sounder, *J. Geophys. Res.*, *112*, D24S50, doi:10.1029/2007JD008709.

Manney, G. L., et al. (2011), Unprecedented Arctic ozone loss in 2011, *Nature*, *478*, 469–475, doi:10.1038/nature10556.

McLinden, C. A., et al. (2000), Stratospheric ozone in 3-D models: A simple chemistry and the cross-tropopause flux, *J. Geophys. Res.*, *105*, 14,653–14,665, doi:10.1029/2000JD900124.

Oetjen, H., et al. (2011), Evaluation of stratospheric chlorine chemistry for the Arctic spring 2005 using modelled and measured OClO column densities, *Atmos. Chem. Phys.*, *11*, 689–703, doi:10.5194/acp-11-689-2011.

Pommereau, J. P., and F. Goutail (1988), O_3 and NO_2 ground-based measurements by visible spectrometry during Arctic winter and spring 1988, *Geophys. Res. Lett.*, *15*, 891–894, doi:10.1029/GL015i008p00891.

Sessler, J., M. P. Chipperfield, J. A. Pyle, and R. Toumi (1995), Stratospheric OClO measurements as a poor quantitative indicator of chlorine activation, *Geophys. Res. Lett.*, *22*, 687–690, doi:10.1029/95GL00202.

Tegtmeier, S., M. Rex, I. Wohltmann, and K. Kruger (2008), Relative importance of dynamical and chemical contributions to Arctic wintertime ozone, *Geophys. Res. Lett.*, *35*, L17801, doi:10.1029/2008GL034250.

Tétard, C., et al. (2009), Simultaneous measurements of OClO, NO_2 and O_3 in the Arctic polar vortex by the GOMOS instrument, *Atmos. Chem. Phys.*, *9*, 7857–7866, doi:10.5194/acp-9-7857-2009.

Tornkvist, K. K., D. W. Arlander, and B. M. Sinnhuber (2002), Ground-based UV measurements of BrO and OClO over Ny-Alesund during winter 1996 and 1997 and Andoya during winter 1998/99, *J. Atmos. Chem.*, *43*, 75–106, doi:10.1023/A:1019905006390.

World Meteorological Organization (2003), Scientific assessment of ozone depletion: 2002, *Global Ozone Res. Monit. Proj. Rep. 50*, Geneva, Switzerland.

C. Adams, E. E. Farahani, K. Strong, K. A. Walker, and X. Zhao, Department of Physics, University of Toronto, 60 St. George St., Toronto, ON M5S 1A7, Canada. (cadams@physics.utoronto.ca)

M. R. Bassford, RAND Europe, Westbrook Centre, Milton Road, Cambridge CB4 1YG, UK.

M. P. Chipperfield and W. Feng, Institute for Climate and Atmospheric Science, School of Earth and Environment, University of Leeds, Leeds LS2 9JT, UK.

W. Daffer and G. Manney, Jet Propulsion Laboratory, California Institute of Technology, 4800 Oak Grove Dr., Pasadena, CA 91109, USA.

J. R. Drummond, Department of Physics and Atmospheric Sciences, Dalhousie University, Halifax, NS B3H 3J5, Canada.

A. Fraser, School of GeoSciences, University of Edinburgh, Crew Building, King's Buildings, West Mains Road, Edinburgh EH9 3JN, UK.

F. Goutail and A. Pazmino, LATMOS, CNRS, 11 Boulevard d'Alembert, F-78280 Guyancourt CEDEX, France.

C. A. McLinden, Environment Canada, 4905 Dufferin St., Toronto, ON M3H 5T4, Canada.

M. Rex, Alfred Wegener Institute for Polar and Marine Research, Telegrafenberg A43, D-14473 Potsdam, Germany.

Auxiliary Material for "Severe 2011 ozone depletion assessed with 11 years of ozone, NO_2, and OClO measurements at 80°N"

C. Adams, K. Strong, X. Zhao, M.R. Bassford, M.P. Chipperfield, W. Daffer, J.R. Drummond, E.E. Farahani, W. Feng, A. Fraser, F. Goutail, G. Manney, C.A. McLinden, A. Pazmino, M. Rex, and Kaley A. Walker

DOAS retrieval of OClO

OClO was retrieved when the GBS high-resolution gratings were used. In 2009 and 2010, instrument problems increased noise, so OClO was not retrieved. Spectra were averaged to a time-resolution of 20-30 minutes prior to data processing in order to improve the signal-to-noise ratio. Data were analyzed using the DOAS technique [*Platt and Stutz*, 2008] in the 350-380 nm wavelength range. The following cross-sections were fit during the DOAS procedure: OClO measured at 204 K [*Wahner et al.*, 1987], ozone measured at 223 K [*Bogumil et al.*, 2003], NO_2 measured at 220 K [*Vandaele et al.*, 1998], O_4 [*Greenblatt et al.*, 1990], BrO measured at 223 K [*Fleischmann et al.*, 2004], and Ring [*Chance and Spurr*, 1997]. A sample OClO DOAS fit for 16 March 2011 (day 75) at evening solar zenith angle (SZA) 90° is shown in Figure S1. The resulting DSCDs between SZA 89-91° from each twilight were averaged. Based on the average DOAS fitting error and the standard deviation of OClO DSCDs between SZA 89-91°, the detection limit was calculated to be 0.6×10^{14} mol/cm^2.

Ozone loss estimates using passive tracer subtraction

Ozone loss was estimated using the passive subtraction method [e.g., *Manney et al.*, 1995; *WMO*, 2003; *Feng et al.*, 2007]. Passive ozone was calculated using the SLIMCAT 3-dimensional offline chemical transport model [*Chipperfield*, 2006], where ozone was treated as a passive dynamical tracer with no chemistry. The SLIMCAT passive ozone columns were calculated daily directly above Eureka and interpolated to the measurement times of the instruments. The DOAS (GBS and SAOZ) instruments sample along a line-of-sight along the path of scattered light to the instrument. When the vortex edge is near Eureka, spatial and temporal differences between SLIMCAT passive ozone and DOAS measurements could lead to errors in the ozone loss estimates.

Agreement between SLIMCAT passive ozone and the DOAS instruments was assessed using December ozonesonde measurements. The DOAS instruments do not operate during polar night, before chemical ozone depletion occurs, and therefore could not be compared directly with the passive ozone. The mean difference and standard error for SLIMCAT passive ozone minus ozonesonde total columns was 89.3±11.4 DU for December 2001-2011. This bias may be due in

part to the coarse vertical resolution in the SLIMCAT model for altitudes below the 350-K potential temperature level [*Feng et al.*, 2007]. Inside the vortex, for spring 1999-2011, the mean difference for GBS (SAOZ) minus ozonesonde total columns was -31±4 DU (-28±3 DU). To correct for these offsets, 119 DU was subtracted from the SLIMCAT passive ozone prior to the analysis.

Figure S2 shows the timeseries of the ozone loss calculations for 1999-2011. Outlying ozone loss estimates may occur when the DOAS and SLIMCAT data sample different airmasses. Furthermore, for large ozone columns, GBS measurements are biased low compared with other instruments [*Adams et al.*, 2012], which can lead to overestimates of ozone loss. For most of the timeseries, the largest ozone loss is observed in 2011. The average ozone loss for 12-20 March 2011 (days 71-79) was 27% (29%) or 99 DU (108 DU), as estimated from GBS (SAOZ) data. During this period, ozone columns were very low and there was evidence of chemical ozone loss above Eureka in supporting datasets, as discussed in Sections 3 and 4 of the paper. The maximum percent ozone loss was calculated from GBS (SAOZ) data on 5 April 2011 (day 95) at 47% (47%) or 250 DU (251 DU).

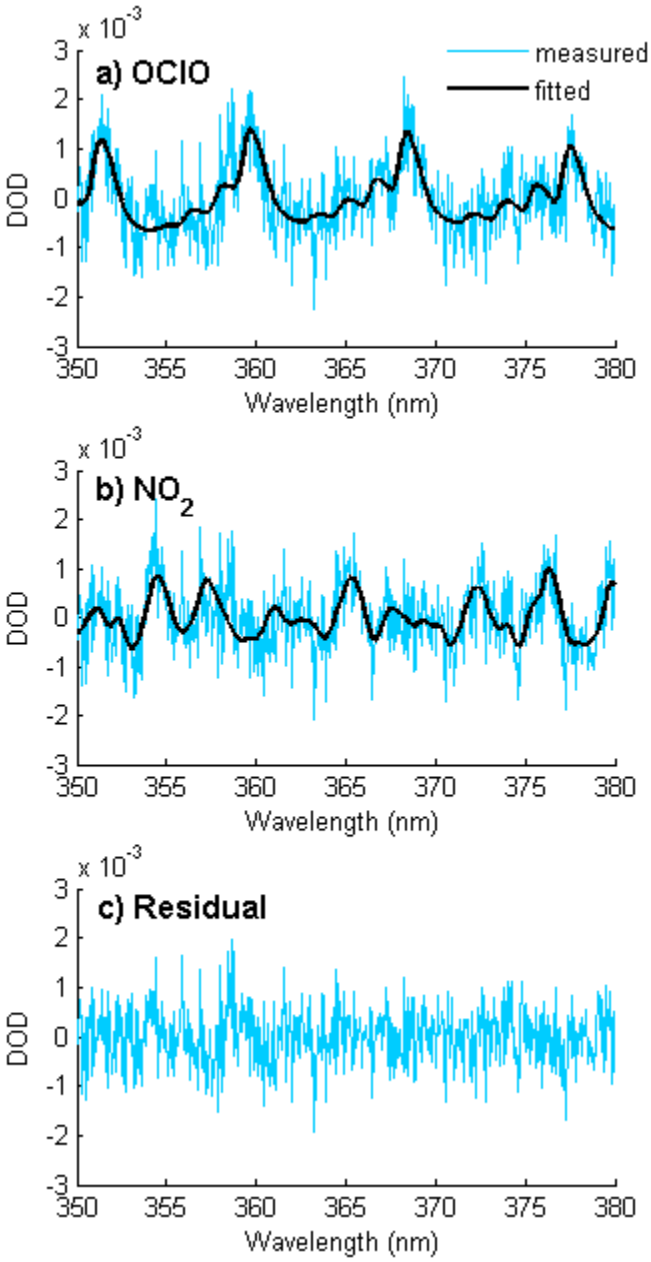

Figure S1. Example of OClO DOAS measurement for SZA 90° on 16 March (day 75) 2011. Measurement (blue) and fit (black) for (a) OClO and (b) NO_2 and (c) residual are shown. DOD = differential optical depth.

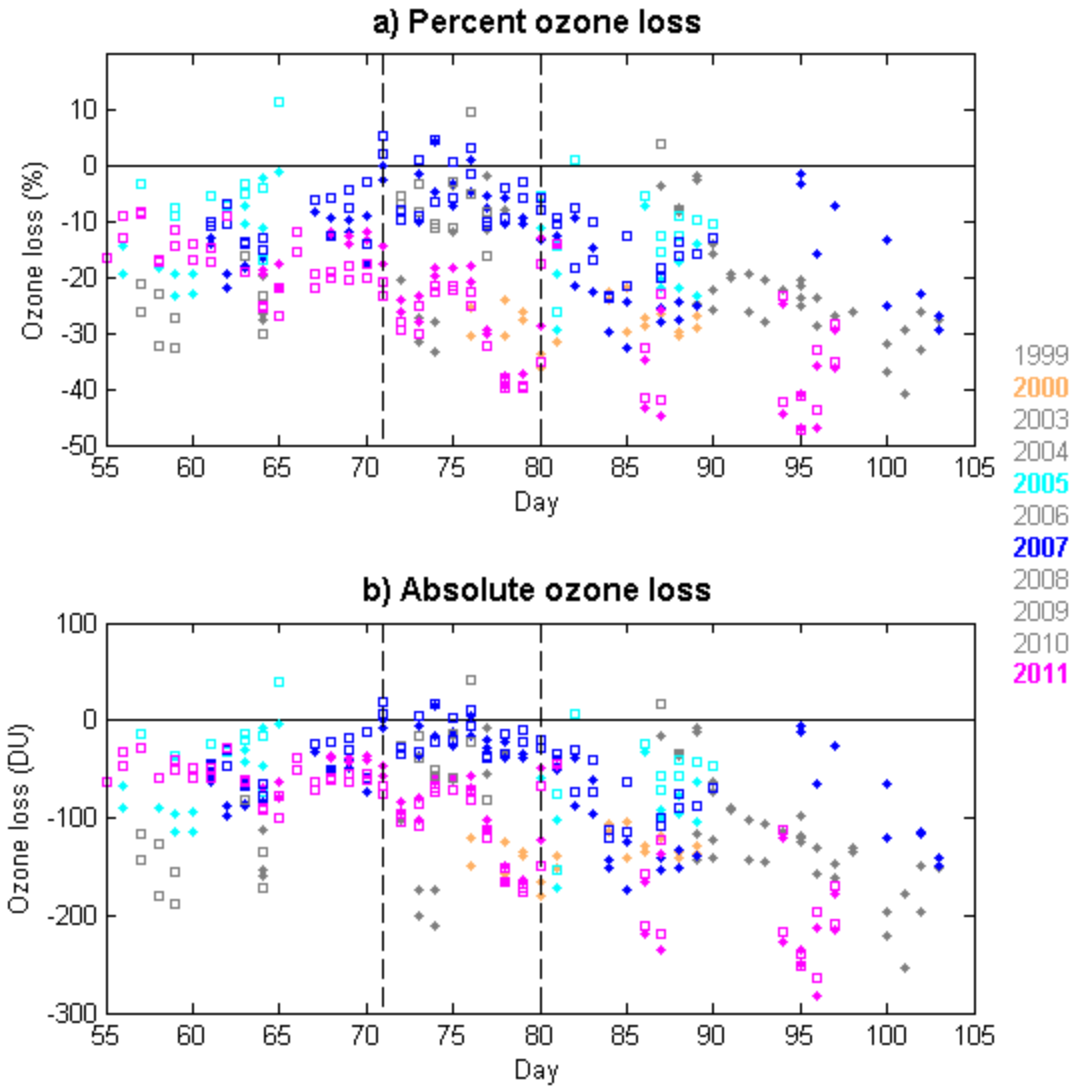

Figure S2. Timeseries of (a) percent ozone loss and (b) absolute ozone loss for 1999-2011 versus day of year for GBS (closed circles) and SAOZ (open squares). Year 2000 is shown in orange, 2005 in cyan, 2007 in blue, 2011 in magenta, and all other years are shown in grey. The black line indicates zero. The black dashed lines enclose days 71-79 (March 11/12 to 19/20).

References

Adams, C., et al. (2012), Validation of ACE and OSIRIS ozone and NO_2 measurements using ground-based instruments at 80°N, *Atmos. Meas. Tech. Discuss.*, *5*, 517-588, doi:10.5194/amtd-5-517-2012.

Bogumil, K., et al. (2003), Measurements of molecular absorption spectra with the SCIAMACHY pre-flight model: instrument characterization and reference data for atmospheric remote-sensing in the 230-2380 nm region, *J. Photochem. Photobiol. A-Chem.*, *157*, 167-184.

Chance, K. V., and R. J. D. Spurr (1997), Ring effect studies: Rayleigh scattering, including molecular parameters for rotational Raman scattering, and the Fraunhofer spectrum, *Appl. Opt.*, *36*, 5224-5230.

Chipperfield, M. P. (2006), New version of the TOMCAT/SLIMCAT off-line chemical transport model: Intercomparison of stratospheric tracer experiments, *Q. J. R. Meteorol. Soc.*, *132*, 1179-1203, doi:10.1256/qj.05.51.

Feng, W., et al. (2007), Large chemical ozone loss in 2004/05 Arctic winter/spring, *Geophys. Res. Lett.*, *34*, L09803, doi:10.1029/2006GL029098.

Fleischmann, O. C., M. Hartmann, J. P. Burrows, and J. Orphal (2004), New ultraviolet absorption cross-sections of BrO at atmospheric temperatures measured by time-windowing Fourier transform spectroscopy, *J. Photochem. Photobiol. A-Chem.*, *168*, 117-132.

Greenblatt, G. D., J. J. Orlando, J. B. Burkholder, and A. R. Ravishankara (1990), Absorption-measurements of oxygen between 330nm and 1140nm, *J. Geophys. Res.-Atmos.*, *95*, 18577-18582.

Manney, G. L., et al. (1995), Lagrangian Transport Calculations Using UARS Data. 2. Ozone, *J. Atmos. Sci.*, *52*, 3069-3081.

Platt, U., and J. Stutz (2008), *Differential Optical Absorption Spectroscopy (DOAS)*, Springer, Germany.

Vandaele, A. C., et al. (1998), Measurements of the NO_2 absorption cross-section from 42 000 cm^{-1} to 10 000 cm^{-1} (238-1000 nm) at 220 K and 294 K, *J. Quant. Spectrosc. Radiat. Transfer*, *59*, 171-184.

Wahner, A., G. S. Tyndall, and A. R. Ravishankara (1987), Absorption cross-sections for OClO as a function of temperature in the wavelength range 240-480 nm, *J. Phys. Chem.*, *91*, 2734-2738.

WMO (2003), Scientific Assessment of Ozone Depletion: 2002, Rep. 50, Global Ozone Research and Monitoring Project, World Meteorological Society, Geneva, Switzerland.